

Enhancement of Dye Adsorption on TiO₂ Surface through Hydroxylation Process for Dye-sensitized Solar Cells

Inseok Jang, Kyungho Song, Jun-Hwan Park, and Seong-Geun Oh*

Department of Chemical Engineering, Hanyang University, Seoul 133-791, Korea

*E-mail: seongoh@hanyang.ac.kr

Received May 29, 2013, Accepted July 3, 2013

To enhance the power conversion efficiency of dye-sensitized solar cell (DSSC), the surface of titanium dioxide (TiO₂) photoelectrode was modified by hydroxylation treatment with NH₄OH solution at 70 °C for 6 h. The NH₄OH solutions of various concentrations were used to introduce the hydroxyl groups on TiO₂ surface. As the concentration of NH₄OH was increased, the short-circuit current density (J_{SC}) value and conversion efficiency of solar cells were increased because the amount of adsorbed dye molecules on TiO₂ surface was increased. As a result of the surface modification to introduce hydroxyl groups, the concentration of adsorbed dye on the TiO₂ surface could be improved up to 32.61% without the changes of morphology, surface area and pore volume of particles. The morphology, the specific surface area, the pore volume and the chemical states of TiO₂ surface were characterized by using FE-SEM, N₂ adsorption-desorption isotherms and XPS measurements. The amount of adsorbed dye and the performance of fabricated cells were analyzed by using UV-Vis absorption spectroscopy and solar simulator.

Key Words : TiO₂, Hydroxylation, Surface modification, Dye adsorption, DSSC

Introduction

The development of DSSC has received a great deal of attraction as a next generation photovoltaic device owing to its outstanding characteristics including reasonable efficiency, low cost, brief fabrication process and flexible cell design.¹⁻⁵ Many researchers have been investigated for the optimization of DSSC consisting of the photosensitizer,⁶⁻⁸ photoelectrode,⁹⁻¹² counter electrode¹³⁻¹⁵ and redox electrolyte¹⁶⁻¹⁸ since the first report of O' Regan and Grätzel in 1991.¹ Among the components, the photoelectrode has been widely studied because it plays important roles in the DSSC, such as the support of dye and the pathway of electrons generated from dyes.¹⁹⁻²¹ Apparently, TiO₂ has most frequently been employed as a photoelectrode material due to its large surface area,^{19,22,23} excellent chemical stability,^{24,25} moderate electron transfer ability^{20,21,26} and wide band gap energy.^{27,28} Also, various materials such as ZnO, SnO₂, CdS and Nb₂O₅ have also been used as an electrode, but none of them exhibited better performance than TiO₂.²⁹⁻³² Several groups have researched morphology control, coating with other material, TiCl₄ treatment of the TiO₂ photoelectrode. Jiu *et al.* reported that the highly crystalline TiO₂ nanorods with lengths of 100-300 nm and diameters of 20-30 nm were synthesized by hydrothermal process to use as a photoelectrode in DSSC. They concluded that high power conversion efficiency of DSSC could be achieved by using one-dimensional TiO₂ due to the rapid transportation of electrons attributed to their morphological advantage.³³ Palomares *et al.* researched the coating of conformal Al₂O₃ overlayer on nanocrystalline TiO₂ films and they demonstrated that the Al₂O₃ overlayer resulted in a retardation of the kinetics of charge recombi-

nation.³⁴ Sommeling *et al.* studied the influence of the TiCl₄ post-treatment on the properties of TiO₂ films. The DSSCs exhibited high value of photocurrents because of the change in thickness, mass, porosity and dye adsorption through TiCl₄ post-treatment.³⁵ Moreover, other researchers have tried to modify the surface of TiO₂ with various materials (*e.g.*, HCl, BaCO₃, KOH, NaOH, *etc.*). Although the various treatments have been suggested to improve the DSSC performance, the relationship between surface modification and DSSC efficiency was not understood clearly.³⁶⁻³⁹ The dye molecules are adsorbed onto the surface of TiO₂ *via* the interaction between hydroxyl groups on TiO₂ surface and the carboxylic anchoring groups residing on dye molecules.²⁻⁶ Generally, the TiO₂ exposed to ambient atmosphere with moisture are partially covered by hydroxyl groups, which are formed in dissociative adsorption process when water molecules break up and form -OH and H⁺ species. The hydroxyl site concentration is typically of the order of 11.6-27.9 μmol/m², which is equivalent to 7.0-16.8 groups/nm².⁴⁰⁻⁴³ However, the TiO₂ particles prepared by thermal process do not have enough hydroxyl groups on the surface. It can be inferred that the dye adsorption can be enhanced by introducing more hydroxyl groups on the surface of TiO₂. In this research, the photovoltaic characteristics of DSSCs fabricated with hydroxylated TiO₂ electrode were investigated. For the enhancement of short-circuit current density (J_{SC}) parameter, the hydroxyl groups were introduced on the TiO₂ surface *via* hydroxylation treatment with NH₄OH, resulting in enhancement of power conversion efficiency of DSSC. The influence of NH₄OH concentration on the modification of TiO₂ surfaces was studied through the observation of changes in morphology, surface area, chemical state, dye adsorption and photo-

voltaic characteristics.

Experimental

Materials. Fluorine-doped tin oxide (FTO, $8.0 \Omega/\text{cm}^2$, thickness: 2.3 mm) glass substrate was purchased from Pilkington. Commercial TiO_2 nanoparticle (P25, average particles size: 25 nm) was obtained from Degussa. *Cis*-bis(isothiocyanato) bis(2,2'-bipyridyl-4,4'-dicarboxylato)-ruthenium(II) bis-tetrabutyl ammonium (N719) as a ruthenium dye sensitizer was provided by Solaronix. As a source of hydroxyl groups, ammonia solution (NH_4OH , 25.0% NH_3 solution) was purchased from Wako. Dibutyl phthalate (99.0%), potassium hydroxide (KOH, 85.0%), titanium tetrakisopropoxide (TTIP, 98.0%) and titanium tetrachloride (TiCl_4 , 99.0%) were purchased from Junsei. Alpha-terpineol (95.0%), ethyl cellulose (10 and 45 cps), 2-propanol (99.9%), ethanol (99.9%) and Surllyn as a spacer (25 μm) were obtained from Kanto, Daejung, J.T. Baker, OCI and DuPont, respectively. Lauric acid (99.0%), acetonitrile (99.8%), *tert*-butanol (99.0%) chloroplatinic acid hexahydrate (H_2PtCl_6 , 99.9%), 1-methyl-3-propylimidazolium iodide (MPII, 98.0%), iodine (I_2 , $\geq 99.9\%$), lithium iodide (LiI, 99.0%) and 4-*tert*-butylpyridine (*t*BP, 96.0%) were purchased from Sigma-Aldrich. All of the chemicals were reagent grades and were used without any further purification. The water used in this research was deionized and double-distilled by the Milli-Q Plus system (Millipore, France) having $18.2 \text{ M}\Omega\cdot\text{cm}$ electrical resistivity at 25 $^\circ\text{C}$.

Preparation of Working Electrode. FTO substrates were cleaned by using acetone and ethanol in an ultrasonic bath for 10 min. Then, a drop of 70 mM TTIP in 2-propanol was placed on the FTO glass by using spin coating followed by heating at 450 $^\circ\text{C}$ for 30 min. A colloidal TiO_2 paste consisting of P25 nanoparticles, lauric acid, alpha-terpineol, dibutyl phthalate and ethyl cellulose was prepared by using ultrasound dispersion method. This TiO_2 paste was placed on the FTO glass *via* doctor blade coating followed by the calcination process at 450 $^\circ\text{C}$ for 30 min. The formed TiO_2 films were soaked in aqueous TiCl_4 (40 mM) solution at 70 $^\circ\text{C}$ for 30 min and washed with water 3 times. Then the obtained films were sintered at 450 $^\circ\text{C}$ for 30 min again.

Hydroxylation Treatment of the TiO_2 Surface. To introduce hydroxyl groups on the prepared TiO_2 surface, the TiO_2 electrodes were immersed in different concentrations of NH_4OH at 70 $^\circ\text{C}$ for 6 h. The resultants were rinsed with water and ethanol and then dried in a vacuum oven at room temperature for 12 h. The untreated and the hydroxylated samples with different concentrations (1, 2 and 4 M) of NH_4OH were identified as UT, 1HT, 2HT and 4HT, respectively.

Dye Adsorption on the TiO_2 Electrode and Fabrication of DSSC. The prepared working electrodes were immersed into a N719 solution (0.3 mM) in a mixed solvent (acetonitrile:*tert*-butanol = 1:1, *v:v*) for 18 h. After the dye adsorption process, the TiO_2 electrodes were rinsed with acetonitrile and dried at 25 $^\circ\text{C}$ for 2 h. In order to prepare Pt counter

electrode, a drop of 10 mM H_2PtCl_6 in 2-propanol was placed on the FTO glass by using spin coating followed by heating at 450 $^\circ\text{C}$ for 30 min. Both electrodes were sealed with Surllyn. Then, the redox electrolyte composed of MPII (0.5 M), I_2 (0.05 M), LiI (0.1 M) and *t*BP (0.05 M) in acetonitrile (5 mL) was introduced into the cell through pre-drilled two holes by capillary action. Finally, the holes were sealed with Surllyn and cover glass.

Characterizations. The thickness of TiO_2 films was measured by using surface profiler (Alpha-step 500). Field emission scanning electron microscopy (FE-SEM, JSM-6700F) instrument was used to observe the morphological change of untreated and hydroxylated samples. Before the analysis of FE-SEM, all samples were coated with platinum by sputtering at 15 mA for 3 min using a coating machine. Brunauer-Emmett-Teller (BET) surface area (S_{BET}) and total pore volume of the samples were determined by N_2 adsorption-desorption isotherms measurement (Belsorp-mini II) at 77 K. X-ray photoelectron spectroscopy (XPS, VG Multilab ESCA 2000 system) was used to investigate the chemical states of samples. UV-Vis spectrophotometer (Agilent 8435, Agilent Technologies) was used to measure the concentration of adsorbed N719 dye molecules on the surface of TiO_2 films. The current-voltage (J-V) characteristics of the DSSCs were analyzed with a solar simulator (300 W Xe source, Newport) with Keithley 2400 sourcemeter under 1-sun illumination (AM 1.5G, $100 \text{ mW}/\text{cm}^2$). For facile analyses of N_2 adsorption-desorption isotherm and XPS, the untreated and the hydroxylated TiO_2 powders were used instead of the TiO_2 films.

Results and Discussion

The thickness and the active area of TiO_2 films on the FTO glass were about 14 μm and 0.25 mm^2 , respectively. To determine the changes of morphological property and surface area of TiO_2 electrodes, the analyses with FE-SEM and N_2 adsorption-desorption isotherms analysis were carried out. Figure 1(a) and (b) show FE-SEM images of UT and 4HT, and the considerable change of morphology was not observed. Also, the surface area and the total pore volume of samples, indicated in Table 1, were not varied significantly. The average values of all samples were $56.26 \pm 0.66 \text{ m}^2/\text{g}$ and $0.145 \pm 0.015 \text{ cm}^3/\text{g}$, approximately. The variations in surface areas and pore volumes with and without hydroxylation process could be negligible, although the specific surface areas and total pore volumes were slightly changed due to the etching by NH_4OH . These results indicate that the surface morphology and the surface area of the TiO_2 were not affected by the hydroxylation treatment.

As shown in Figure 2 and Figure 3, the chemical states of samples were observed by using XPS. The XPS survey spectra of UT and 4HT were shown in Figure 2(a). Both survey spectra contain Ti, O and C elements, which are assigned as Ti 2p, O 1s and C 1s, respectively.⁴⁴ The trace amount of carbon peak is ascribed to the adventitious hydrocarbon from the XPS instrument itself. Figure 2(b) shows

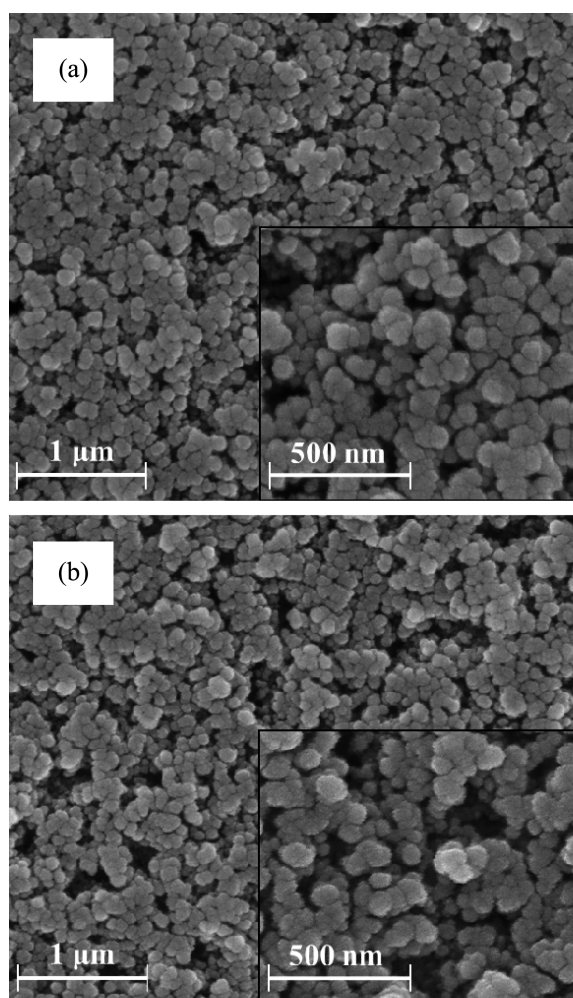


Figure 1. FE-SEM images of untreated (a) and hydroxylated with NH₄OH concentration (4 M) (b) TiO₂ electrodes and inset indicates their high-resolution images.

the high-resolution XPS spectra of Ti 2p region of the samples. The splitting width between Ti 2p_{1/2} and Ti 2p_{3/2} of all samples was 5.7 eV, indicating a normal state of Ti⁴⁺.⁴⁴ When compared with the Ti 2p peaks of UT, those of modified TiO₂ with NH₄OH were shifted to lower binding energy and their intensities became smaller as the concentration of NH₄OH solution was increased. It means that the more O atoms were chemically adsorbed on the TiO₂ surface than the Ti atom.⁴⁵ After the hydroxylation with 4 M concentration of NH₄OH solution, any N 1s peak was not observed at around 400 eV (not shown in this paper).⁴⁴ This shows that NH₃ in this hydroxylation system was completely eliminated during a vacuum drying at room temperature for 12 h. From this result, we could focus on the effect of surface modification with hydroxyl groups on the TiO₂ surface without considering the change of energy level by doped N.

Figure 3 indicates the high-resolution XPS of O 1s region of untreated and hydroxylated samples. The O 1s curves of samples were fitted with the distribution of three peaks located at 533.2 ± 0.3, 531.6 ± 0.2 and 529.6 ± 0.3 eVs, assigned as the adsorbed water molecules, hydroxyl groups

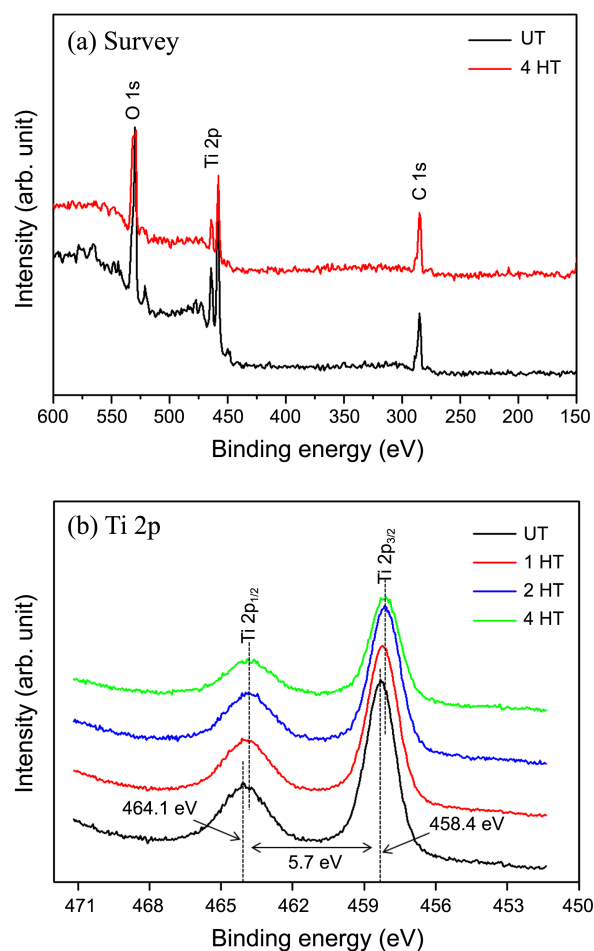


Figure 2. XPS survey spectra (a) and high-resolution spectra of Ti 2p region (b) of untreated and hydroxylated TiO₂ electrodes.

Table 1. Estimation of surface area, total pore volume and peak ratio of untreated and hydroxylated TiO₂ electrodes

Sample	Surface area ^a (m ² /g)	Total pore volume ^b (cm ³ /g)	-OH/O ²⁻ ratio ^c
UT	56.92	0.13	0.09
1HT	56.08	0.16	0.32
2HT	55.60	0.15	0.92
4HT	55.84	0.16	1.47

^aevaluated by BET method. ^bdetermined from adsorption branch using the BJH model. ^ccalculated through integration of peak area from O 1s

(-OH, surface) and oxide (O²⁻, bulk) species, respectively.^{40,44-47} As shown in Figure 3(a), the two peaks at 531.6 and 529.8 eVs are attributed to hydroxyl groups and oxide were observed in UT. The oxide peak was predominant over hydroxyl peak, and the peak at around 533.0 eV ascribed to water adsorption on the TiO₂ surface was barely observed. Because most water adsorbed on the TiO₂ surface was removed during the thermal process at 450 °C.⁴⁰⁻⁴³ On the other hand, the water peak was observed in hydroxylated samples as illustrated in Figure 3(b), (c) and (d). These results were caused by the hydrogen bonding between water molecules from NH₄OH solution and hydroxyl groups on

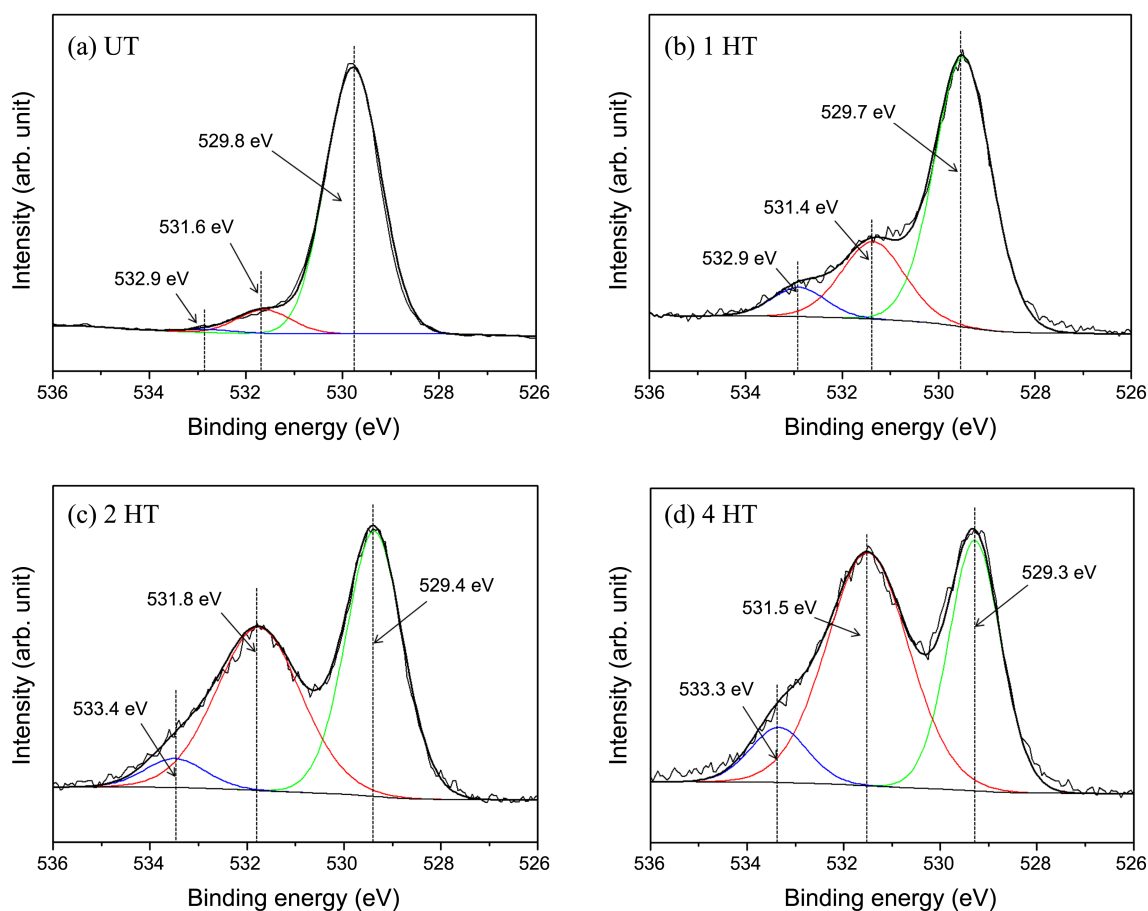


Figure 3. High-resolution XPS spectra of O 1s region of untreated (a) and hydroxylated (b-d) TiO₂.

the surface of hydroxylated TiO₂ through the hydroxylation process. In other words, it means that the hydroxyl groups were introduced successfully on the surface of TiO₂ in this hydroxylation system. In addition, as the higher concentration of NH₄OH was introduced on the TiO₂ surface in this hydroxylation system, the –OH/O^{2–} peak ratio was increased as listed in Table 1. The values of –OH/O^{2–} of ratio of untreated and hydroxylated samples in Figure 3(a), (b), (c) and (d) were 0.08, 0.32, 0.92 and 1.47, respectively. From these results, it is expected that the more amount of –OH groups were chemi-adsorbed on the surface of TiO₂ as the higher NH₄OH concentration was used.

In order to investigate into the effect of hydroxylation process on the amount of adsorbed N719 dye, the dye molecules on the surface of untreated and hydroxylated TiO₂ films were desorbed into 4 mM of KOH in a mixed solvent (water:ethanol = 1:1, v:v). Then, UV-Vis absorption spectra of the resultant solutions were measured to estimate the concentration of adsorbed dye molecules (Figure 4(a)). The concentration of adsorbed dye was calculated by using the Beer-Lambert law, $A = \epsilon lc$, where A is the intensity of the UV-Vis absorption spectra at 515 nm, ϵ is the molar extinction coefficient of N719 at 515 nm determined to be 14,100/M cm, l is the path length of the light beam and c is the dye molecular concentration.⁴⁸ The calculated dye adsorption values are shown in Figure 4(b) and summarized in Table 2.

The amount of adsorbed dye molecules per unit active area for the 1HT, 2HT and 4HT were established to be 6.33, 6.60 and 7.32×10^{-8} mol/cm², which is larger than that of UT (5.52×10^{-8} mol/cm²). This result is consistent with a trend of the above explained XPS data. Through this process, the concentration of adsorbed dye could be improved up to 32.61%. It indicates that the reason of improvement dye adsorption in this hydroxylation process was not the effects of morphological characteristics and surface area but surface modification with hydroxyl groups. The chemical adsorption of N718 dye molecules on TiO₂ surface is illustrated in Figure 5. As shown in Figure 5(a), the general fabrication process of DSSCs involves the thermal processes above 450 °C (e.g., TiO₂ phase transition, sintering, TiCl₄ treatments, and so on). A number of hydroxyl groups on the TiO₂ surface were reduced during the heat treatment.^{40–42} However, through the hydroxylation treatment with NH₄OH solution, the hydroxyl groups can be introduced without the changes in the morphology of surface, the surface area and the total pore volume of the TiO₂ (Figure 5(b)). It results in the enhancement of dye adsorption because the dye could be adsorbed *via* interaction between carboxylic anchoring groups residing on N719 and hydroxyl groups on the TiO₂ surface as illustrated in Figure 5(c).

To verify the influence of dye amount adsorbed on the TiO₂ for the improvement in the performance of DSSCs, the

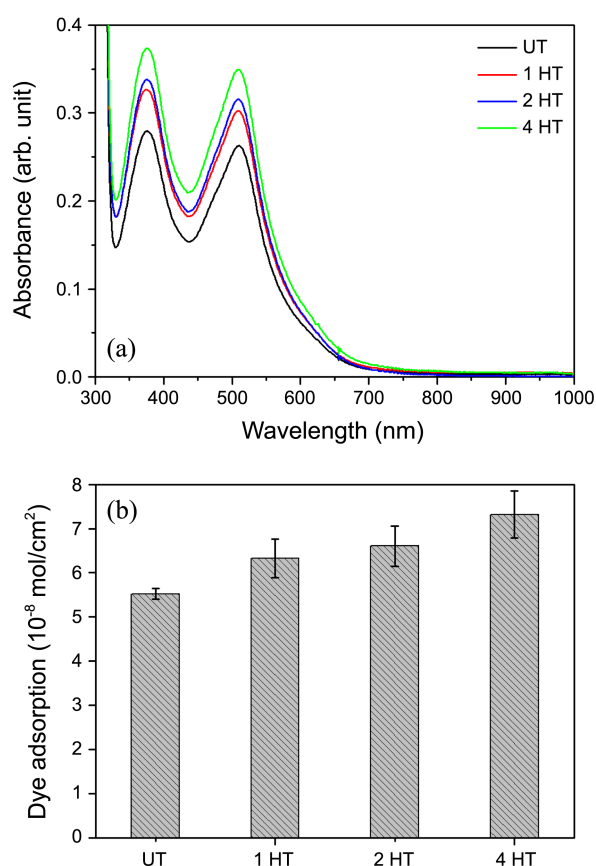


Figure 4. UV-Vis absorption spectra of the solutions containing dye detached from each TiO₂ electrode (a) and the amount of dye adsorbed on untreated and hydroxylated TiO₂ electrodes (b).

Table 2. N719 dye adsorption values of untreated and hydroxylated TiO₂ electrodes

Sample	Dye adsorption (10 ⁻⁸ mol/cm ²)	Standard deviation (10 ⁻⁸ mol/cm ²)	Enhancement (%)
UT	5.52	0.13	-
1HT	6.33	0.44	14.67
2HT	6.60	0.45	19.57
4HT	7.32	0.53	32.61

J-V characteristics of the cells fabricated with untreated and hydroxylated TiO₂ electrodes were measured under standard light irradiation. The results are shown in Figure 6 and summarized in Table 3, in detail. Except for the short-circuit current density (J_{SC}), the open-circuit voltage (V_{OC}) and fill factor (FF) of all DSSCs were not significantly changed. The cell prepared with untreated electrode showed the lowest power conversion efficiency because of the low J_{SC} . On the other hand, the higher power conversion efficiencies were observed when the cells were fabricated with hydroxylated films. Also, the efficiency of cell was enhanced as the concentration of NH₄OH was increased for the surface modification process. These results were caused by the increase in the dye amount adsorbed on the surface of TiO₂ inducing the improvement of J_{SC} value.⁴⁹ In other words, the enhan-

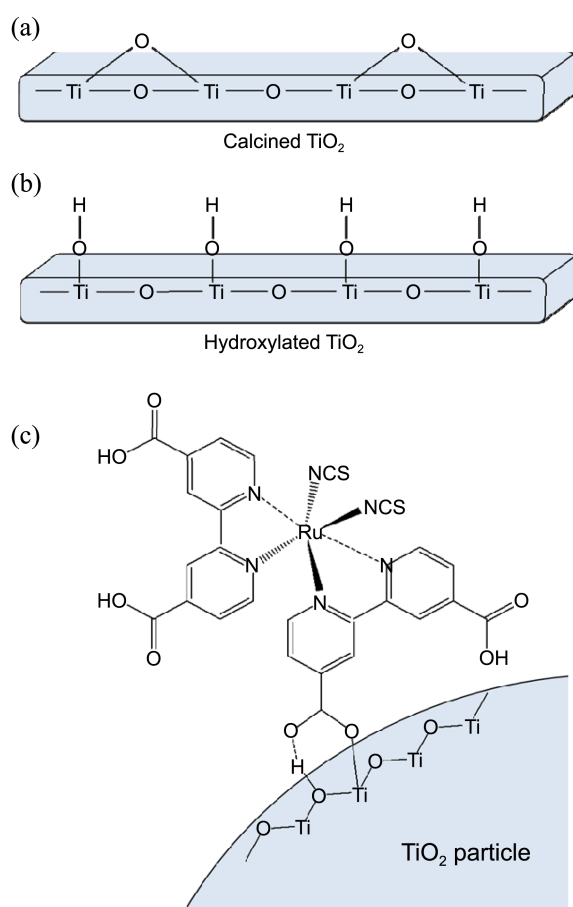


Figure 5. Surfaces of TiO₂ electrodes before and after hydroxylation treatment (a, b), and after the adsorption of N719 dye (c).

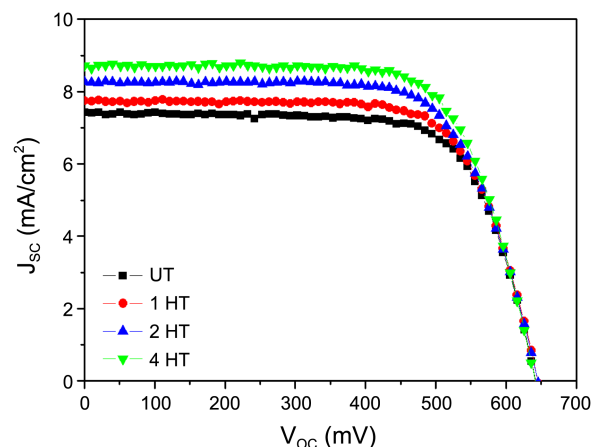


Figure 6. *J-V* curves of the DSSCs prepared using untreated and hydroxylated TiO₂ electrodes.

Table 3. Photovoltaic parameters of fabricated DSSCs with untreated and hydroxylated TiO₂ electrodes

Sample	J_{SC} (mA/cm ²)	V_{OC} (mV)	FF (%)	Efficiency (%)
UT	7.4	642.1	71.1	3.4
1HT	7.8	645.2	71.3	3.5
2HT	8.3	645.5	69.8	3.7
4HT	8.7	641.5	70.6	4.0

cement in the power conversion efficiency of DSSCs could be accomplished by increasing the J_{SC} values through the surface modification of TiO₂ films with hydroxyl groups. From these results, it was confirmed that the more adsorbed dye molecules *via* hydroxylation process using the higher concentration of NH₄OH solution resulted in the increases of the J_{SC} values and the power conversion efficiency of DSSCs.

Conclusion

In summary, the hydroxyl group was successfully chemisorbed on the surface of TiO₂ film *via* surface modification process with NH₄OH and the amount of treated hydroxyl group could be controlled by varying the NH₄OH concentration without the changes of morphological property, specific surface area and total pore volume. As the number of the hydroxyl groups was increased, the more amount of N719 dye was attached on the TiO₂ surface because of the stronger chemical bonding between the increased number of hydroxyl groups and the carboxyl anchoring groups in dye. The amount of adsorbed dye on hydroxylated TiO₂ electrode could be improved up to 32.61%, resulting in the enhancement of the J_{SC} and the power conversion efficiency of DSSCs.

Acknowledgments. This work was supported by the National Research Foundation of Korea (NRF) grant funded by the Korea government (MSIP) for the Center for Next Generation Dye-sensitized Solar Cells (No. 2008-0061903).

References

- O'Regan, B.; Grätzel, M. *Nature* **1991**, *353*, 737.
- Nazeeruddin, M. K.; Kay, A.; Rodicio, I.; Humphrey-Baker, R.; Müller, E.; Liska, P.; Vlachopoulos, N.; Grätzel, M. *J. Am. Chem. Soc.* **1993**, *115*, 6382.
- Hagfeldt, A.; Grätzel, M. *Chem. Rev.* **1995**, *95*, 49.
- Hagfeldt, A.; Grätzel, M. *Acc. Chem. Res.* **2000**, *33*, 269.
- Grätzel, M. *Prog. Photovolt. Res. Appl.* **2000**, *8*, 171.
- Zaban, A.; Ferrere, S.; Gregg, B. A. *J. Phys. Chem. B* **1998**, *102*, 452.
- Nazeeruddin, M. K.; Klein, C.; Liska, P.; Grätzel, M. *Coord. Chem. Rev.* **2005**, *249*, 1460.
- Giribabu, L.; Kumar, C. V.; Reddy, V. G.; Reddy, P. Y.; Rao, C. S.; Jang, S. R.; Yum, J. H.; Nazeeruddin, M. K.; Grätzel, M. *Sol. Energ. Mat. Sol. C* **2007**, *91*, 1611.
- Kim, H. S.; Lee, C.-R.; Jang, I. H.; Kang, W.; Park, N. G. *Bull. Korean Chem. Soc.* **2012**, *33*, 670.
- Hosono, E.; Fujihara, S.; Kimura, T. *Electrochim. Acta* **2004**, *49*, 2287.
- Liao, J. Y.; Ho, K. C. *Sol. Energ. Mat. Sol. C* **2005**, *86*, 229.
- Gao, Y.; Nagai, M. *Langmuir* **2006**, *22*, 3936.
- Li, Q.; Wu, J.; Tang, Q.; Lan, Z.; Li, P.; Lin, J.; Fan, L.; *Electrochem. Commun.* **2008**, *10*, 1299.
- Imoto, K.; Takahashi, K.; Yamaguchi, T.; Komura, T.; Nakamura, J. I.; Murata, K. *Sol. Energ. Mat. Sol. C* **2003**, *79*, 459.
- Koo, B. K.; Lee, D. Y.; Kim, H. J.; Lee, W. J.; Song, J. S.; Kim, H. *J. Electroceram.* **2006**, *17*, 79.
- Kawano, R.; Matsui, H.; Matsuyama, C.; Sato, A.; Susan, M. A. B. H.; Tanabe, N.; Watanabe, M. *J. Photochem. Photobiol. A* **2004**, *164*, 87.
- Suri, P.; Mehra, R. M. *Sol. Energ. Mat. Sol. C* **2007**, *91*, 518.
- Berginc, M.; Krašovec, U. O.; Jankovec, M.; Topič, M. *Sol. Energ. Mat. Sol. C* **2007**, *91*, 821.
- Chen, D.; Huang, F.; Cheng, Y. B.; Caruso, R. A. *Adv. Mater.* **2009**, *21*, 2206.
- Hannappel, T.; Burfeindt, B.; Storck, W.; Willig, F. *J. Phys. Chem. B* **1997**, *101*, 6799.
- Wang, G.; Wang, Q.; Lu, W.; Li, J. *J. Phys. Chem. B* **2006**, *110*, 22029.
- Negishi, N.; Takeuchi, K.; Ibusuki, T. *J. Mat. Sci.* **1998**, *33*, 5789.
- Tian, G.; Fu, H.; Jing, L.; Xin, B.; Pan, K. *J. Phys. Chem. C* **2008**, *112*, 3083.
- Haile, S. M.; Staneff, G.; Ryu, K. H. *J. Mat. Sci.* **2001**, *36*, 1149.
- Hosono, E.; Fujihara, S.; Kakiuchi, K.; Imai, H. *J. Am. Chem. Soc.* **2004**, *126*, 7790.
- Rehm, J. M.; McLendon, G. L.; Nagasawa, Y.; Yoshihara, K.; Moser, J.; Grätzel, M. *J. Phys. Chem.* **1996**, *100*, 9577.
- O'Regan, B.; Schwartz, D. T. *J. Appl. Phys.* **1996**, *80*, 4749.
- Grätzel, M. *J. Sol-Gel Sci. Technol.* **2001**, *22*, 7.
- Martinson, A. B. F.; Elam, J. W.; Hupp, J. T.; Pellin, M. *J. Nano Lett.* **2007**, *7*, 2183.
- Dinh, N. N.; Bernard, M. C.; Goff, A. H. L.; Stergiopoulos, T.; Falaras, P. *C. R. Chimie* **2006**, *9*, 676.
- Lin, S. C.; Lee, Y. L.; Chang, C. H.; Shen, Y. J.; Yang, Y. M. *Appl. Phys. Lett.* **2007**, *90*, 143517.
- Ghosh, R.; Brennaman, M. K.; Uher, T.; Ok, M. R.; Samulski, E. T.; McNeil, L. E.; Meyer, T. J.; Lopez, R. *ACS Appl. Mater. Interfaces* **2011**, *3*, 3929.
- Jiu, J.; Isoda, S.; Wang, F.; Adachi, M. *J. Phys. Chem. B* **2006**, *110*, 2087.
- Palomares, E.; Clifford, J. N.; Haque, S. A.; Lutz, T.; Durrant, J. R. *Chem. Commun.* **2002**, 1464.
- Sommeling, P. M.; O'Regan, B. C.; Haswell, R. R.; Smit, H. J. P.; Bakker, N. J.; Smits, J. J. T.; Kroon, J. M.; van Roosmalen, J. A. M. *J. Phys. Chem. B* **2006**, *110*, 19191.
- Jung, H. S.; Lee, J. K.; Lee, S.; Hong, K. S.; Shin, H. *J. Phys. Chem. C* **2008**, *112*, 8476.
- Park, K. H.; Jin, E. M.; Gu, H. B.; Shim, S. E.; Hong, C. K. *Mater. Lett.* **2009**, *63*, 2208.
- Kim, C.; Kim, J. T.; Kim, H.; Park, S. H.; Son, K. C.; Han, Y. S. *Curr. Appl. Phys.* **2010**, *10*, e176.
- Jeong, H.; Lee, Y.; Kim, Y.; Kang, M. *Korean J. Chem. Eng.* **2010**, *27*, 1462.
- McCafferty, E.; Wightman, J. P. *Surf. Interface Anal.* **1998**, *26*, 549.
- Tamura, H.; Tanaka, A.; Mita, K.; Furuichi, R. *J. Colloid Interf. Sci.* **1999**, *209*, 225.
- Tamura, H.; Mita, K.; Tanaka, A.; Ito, M. *J. Colloid Interf. Sci.* **2001**, *243*, 202.
- Harju, M.; Mäntylä, T.; Vähä-Heikkilä, K.; Lehto, V. P. *App. Surf. Sci.* **2005**, *249*, 115.
- Moulder, J. F.; Stickle, W. F.; Sobol, P. E.; Bomben, K. D. *Handbook of X-ray Photoelectron Spectroscopy*; Perkin-Elmer Corp: Eden Prairie, MN, 1992.
- Jung, C. K.; Bae, I. S.; Song, Y. H.; Kim, T. K.; Vlcek, J.; Musil, J.; Boo, J. H. *Surf. Coat. Technol.* **2005**, *200*, 534.
- Yu, J.; Zhao, X.; Du, J.; Chen, W. *J. Sol-Gel Sci. Technol.* **2000**, *17*, 163.
- Erdem, B.; Hunsicker, R. A.; Simmons, G. W.; Sudol, E. D.; Dimonie, V. L.; El-Aasser, M. S. *Langmuir* **2001**, *17*, 2664.
- Wang, Z. S.; Kawachi, H.; Kashima, T.; Arakawa, H. *Coord. Chem. Rev.* **2004**, *248*, 1381.
- Kang, S. H.; Choi, S. H.; Kang, M. S.; Kim, J. Y.; Kim, H. S.; Hyeon, T.; Sung, Y. E. *Adv. Mater.* **2008**, *20*, 54.